UNIVERSIDAD NACIONAL DE COLOMBIA
SEDE MEDELLÍN
FACULTAD DE MINAS

DYNA
http://dyna.medellin.unal.edu.co/

Structural and magnetic properties of the $Bi_{1-x}Lu_xFeO_3$ (x = 0.00, 0.02 and 0.04) system

Angela Maria Morales-Rivera [a], Iván Fernando Betancourt-Montañez[a], Segundo Augustín Martínez-Ovalle [b], Óscar Hernando Pardo-Cuervo[c], Julieth Alexandra Mejía-Gómez[d], Sully Segura-Peña [e], César Armando Ortíz-Otálora[f] & Carlos Arturo Parra-Vargas

[a] *Grupo GFM, Facultad de Ciencias, Universidad Pedagógica y Tecnológica de Colombia, Tunja, Boyacá, Colombia. angela.moralesrivera@uptc.edu.co, ivanbetancourt5@gmail.com, carlos.parra@uptc.edu.co*
[b] *Grupo FINUAS, Facultad de Ciencias, Universidad Pedagógica y Tecnológica de Colombia, Tunja, Boyacá, Colombia. s.agustin.martinez@uptc.edu.co*
[c] *Grupo de Catálisis UPTC, Facultad de Ciencias, Universidad Pedagógica y Tecnológica de Colombia, Tunja, Boyacá, Colombia. oscarhernando.pardo@uptc.edu.co*
[d] *Grupo GIFAM, Facultad de Ciencias, Universidad Antonio Nariño, Tunja, Boyacá, Colombia. juliethmejia@uan.edu.co*
[e] *Grupo de Ciencia Aplicada Tunja, Departamento de Ciencias Básicas, Universidad Santo Tomás, Tunja, Boyacá, Colombia. sully.segura01@usantoto.edu.co*
[f] *Grupo GSEC, Facultad de Ciencias, Universidad Pedagógica y Tecnológica de Colombia, Tunja, Boyacá, Colombia. cesar.ortiz@uptc.edu.co*

Received: November 14th, 2019. Received in revised version: August 11th, 2020. Accepted: August 24th, 2020.

Abstract
This paper reports the synthesis and characterization of $Bi_{1-x}Lu_xFeO_3$ (x = 0.00, 0.02, and 0.04) produced by solid-state reaction, in order to evaluate the influence of lutetium on the structural and magnetic properties of bismuth ferrite ($BiFeO_3$). The samples were characterized by X-ray diffraction (XRD), scanning electron microscopy (SEM), energy-dispersive X-ray spectroscopy (EDX), and magnetic analysis by vibrating sample magnetometer (VSM) in the temperature range from 50 to 320 K. The obtained results allowed confirming the formation of crystalline materials of rhombohedral structure, space-group *R3c* (161), defined morphology and particle sizes between 2.25 and 4.50 µm. The Lu^{3+} insertion in the structure caused an increase in magnetization, purity of $BiFeO_3$, and a decrease in the synthesis temperature as compared with the reported in the literature.

Keywords: bismuth ferrite; lutetium; magnetic properties.

Propiedades estructurales y magnéticas del sistema $Bi_{1-x}Lu_xFeO_3$ (x = 0.00, 0.02 y 0.04)

Resumen
Este artículo reporta la síntesis y caracterización de $Bi_{1-x}Lu_xFeO_3$ (x = 0.00, 0.02 and 0.04) producido por reacción de estado sólido, con el fin de evaluar la influencia del catión lutecio sobre las propiedades estructurales y magnéticas de la ferrita de bismuto ($BiFeO_3$). Las muestras fueron caracterizadas por difracción de rayos X (DRX), microscopia electrónica de barrido (MEB), espectroscopia de energía dispersiva de rayos X (EDX) y análisis magnético por medio de magnetometría de muestra vibrante (VSM) en un rango de temperatura de 50 a 320 K. Los resultados obtenidos permitieron confirman la formación de materiales cristalinos de estructura romboédrica, grupo espacial *R3c* (161), de morfología definida y tamaños de partícula entre 2.25 y 4.50 µm. La inserción de Lu^{3+} en la estructura provocó un aumento en la magnetización, la pureza de $BiFeO_3$ y una disminución en la temperatura de síntesis en comparación con lo reportado en la literatura.

Palabras clave: ferita de bismuto; lutecio; propiedades magnéticas.

How to cite: Morales-Rivera, A.M, Betancourt-Montañez, I.F, Martínez-Ovalle, S.A, Pardo-Cuervo, O.H, Mejía-Gómez, J.A, Segura-Peña, S, Ortíz-Otálora, C.A. and Parra-Vargas, C.A, Structural and magnetic properties of the Bi1-xLuxFeO3 (x = 0.00, 0.02 and 0.04) system. DYNA, 87(215), pp. 84-89, October - December, 2020.

1. Introduction

Nowadays, studies are orienting towards the development of new multifunctional materials with properties such as ferroelectricity, ferromagnetism, and multiferrosity. Bismuth ferrite ($BiFeO_3$) is a good example of multifunctional materials,since it has high Curie and Néel temperatures (T_C = 1083 K, T_N = 673 K) [1,2]. Besides, it exhibits ferromagnetic (FM), ferroelectric (FE), and ferroelasticity properties based on magnetization, electric polarization, and elastic effort, respectively [3]. These properties make the $BiFeO_3$ a material of great interest in the scientific field. Although some materials ($BiMnO_3$, $TbMnO_3$, $TbMn_2O_5$, $YMnO_3$, $LuFeO_4$, and $Ni_3B_7O_{13}$) show similar properties, only bismuth ferrite presents ferroelectricity and antiferromagnetism at room temperature [4,5].

Bismuth ferrite exhibits a G-type antiferromagnetic (G-AFM) ordering with a long-wavelength period ~62 nm, weak ferromagnetism and linear magnetoelectric effect [6]. In addition, it has a bad circuit ferroelectric, and polarization remnants due to charge defects linked to oxygen vacancies [7].

Recent studies have focused on improving the magnetic properties of bismuth ferrites through smaller particle sizes and avoiding the secondary phases. The bismuth substitution for rare earth elements such as samarium (Sm) [8], gadolinium (Gd) [9], neodymium (Nd) [10,11], holmium (Ho) [12] dysprosium (Dy) [13], praseodymium (Pr) [14] and lanthanum (La) [15], which allowed high densification and the elimination of not multiferroic phases [16], as well as their application in spintronics devices like field-effect transistors, electrical switching, nanoelectronics, magnetoelectric random access memories (MERAMs) and sensors [17].

In this paper $Bi_{1-x}Lu_xFeO_3$ system (x = 0.00, 0.02, and 0.04) was produced by the solid-state reaction method and characterized, studying the effect of lutetium doping on its morphological, structural, and magnetic properties.

2. Materials and methods

The $Bi_{1-x}Lu_xFeO_3$ (x=0.00, 0.02 and 0.04) samples were synthesized by solid-state reaction method. Stoichiometric amounts of the oxides Bi_2O_3, Fe_2O_3, and Lu_2O_3 with 99.9% purity were dried, weighed, calcined at 750 °C for 9 h and sintered at 800 °C for 9 h, with intermediate milling and pellet pressing.

The solids obtained were characterized by X-ray diffraction (XRD), using the DRX equipment PANalytical X'Pert PRO-MPD equipped with an Ultra-fast X'Celerator detector in Bragg-Brentano arrangement, using Cu Kα radiation (λ = 1.54060 Å) from 20° to 80° 2 Theta. The results were refined with the GSAS and PCW software. The morphological properties were evaluated by scanning electron microscopy (SEM) with FEI Quanta 200-r equipment. Finally, the magnetic characterization was carried out in a VersaLab-type magnetometer of vibrating sample from Quantum Design company, the measurements were made in the temperature range from 50 - 320 K and magnetic fields from -30 to 30 kOe. The zero-field cooled (ZFC) method was used to measure the magnetization as a function of temperature (at 1000 Oe).

3. Results and discussion

The diffractograms of the $Bi_{1-x}Lu_xFeO_3$ system are in Fig. 1. BFO, BFO2 and BFO4 are x = 0.00, 0.02 and 0.04, respectively. XRD signals revealed high crystallinity of the solids obtained. The patterns analysis evidenced the majority formation of bismuth ferrite ($BiFeO_3$) with file code JCPDS-01-086-1518, rhombohedral structure, and space-group *R3c* (161), with preferential orientation on the (1 1 0) plane and the secondary phase $Bi_2Fe_4O_9$ with file code JCPDS- 00-025-0090, orthorhombic structure, space-group *Pbam* (55) with a preferential orientation on the (1 2 1) plane [17]. The formation of the secondary phase was can be attributed to the reduced range of thermal stability that $BiFeO_3$ presents. This decomposition is associated with high bismuth volatility, considering the synthesis temperature [18]. The XRD analysis shows that the secondary phase decreases when the percentage of lutetium doping increases, which stabilizes the main crystalline phase [19,20]. These results are in accordance with the reported by other authors [21].

Fig. 1 (b) shows the zoom-in of the 31º-33º 2 Theta range. A shifting toward smaller angles was observed, which indicated the structural distortion generated by the ionic radius difference of substituent cation, which shows the correct lutetium doping in bismuth ferrite [22,23].

Rietveld refinement allowed determining the lattice parameters (Table 1). Fig. 2 shows the refined X-ray diffractogram of BFO2, a high correlation between the experimental and theoretical data was observed, with preferential orientation in the plane (1 1 0) located at 32o 2 Theta and Fig. 2 (b) shows the cell unit obtained with PCW software, which is characteristic of these ferrites [24].

Fig. 3 shows the micrographs obtained for each material, particle size distribution was determined using the image J. software. In the micrographs can be observed the presence of interconnected particles with well-defined edges, irregular shapes and sizes. Particle sizes were between 2.25 and 4.50 μm, the values are attributable to lutetium insertion at the A site of the ferrite. These results were correlated with the data obtained by Rietveld refinement (Fig. 4). Lu^{3+} cation has an ionic radius of 25% less than Bi^{3+} cation, causing the unit-cell volume reduction and the decrease in particle size [25]. Additionally, doping can suppress oxygen vacancy concentration, which leads to smaller particle sizes. This behavior is common in the substitution of rare earth elements into the bismuth ferrite structure [26].

Magnetic hysteresis loops, obtained at 50 and 200 K (Fig. 5), exhibits typical magnetism of bismuth ferrites systems. These magnetic properties are associated with unpaired electrons on the Fe^{3+} *d*-orbital, located at the B site. Remnant magnetization values increase with the higher x values (Table

2), which is due to the ionic radium of Lu^{3+} is lower compared to the one for Bi^{3+}. Therefore, doping affects the bonds between Bi-O and Fe-O [27-28].

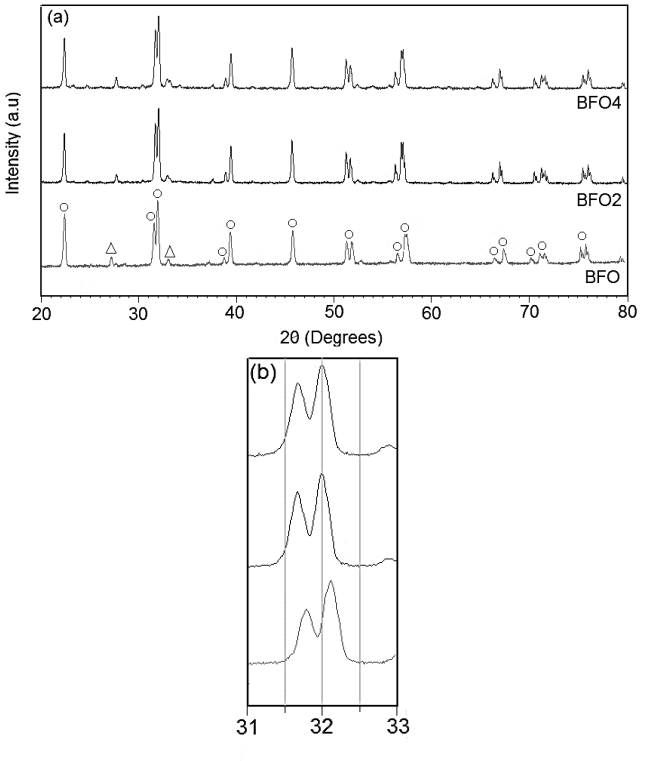

Figure 1. (a) X-ray diffractograms of the $Bi_{1-x}Lu_xFeO_3$ samples: **O** main phase ($BiFeO_3$), **Δ** $Bi_2Fe_4O_9$ phase, and (b) zoom-in of the main signals.
Source: The Authors.

Table 1.
Lattice parameters obtained from the Rietveld refinement.

x	$a = b$ (Å)	c (Å)	V (Å)	R *(%)*	χ^2
0.00	5.578(8)	13.869(7)	373.840	10.08	2.1
0.02	5.578(3)	13.869(4)	373.772	14.95	3.4
0.04	5.575(9)	13.860(1)	373.194	16.13	3.6

Source: The Authors.

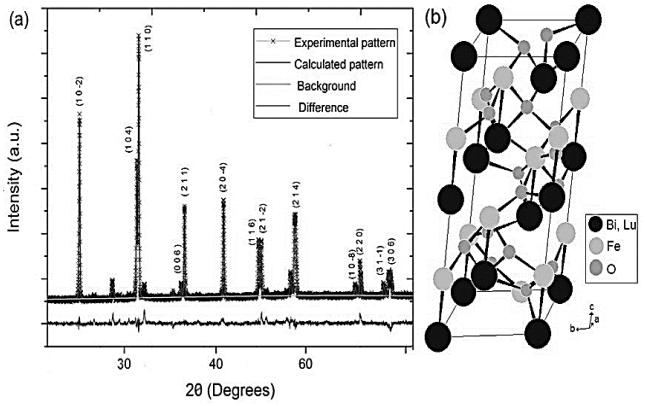

Figure 2. (a) Results of the Rietveld refinement of BFO2 sample and (b) unit cell obtained from experimental X-ray data and plotted with PCW software.
Source: The Authors.

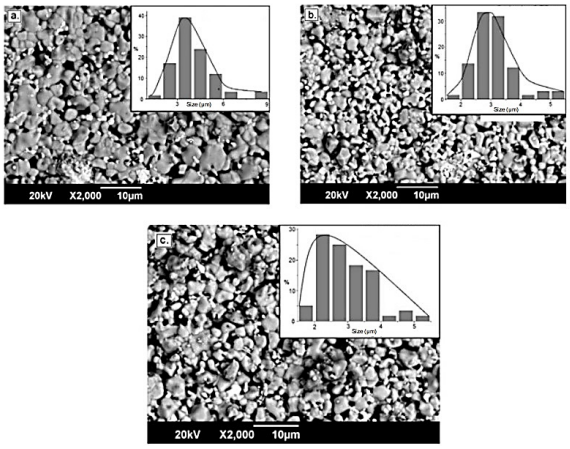

Figure 3. Scanning electron microscopy images and particle size distribution for (a) BFO, (b) BFO2, and (c) BFO4.
Source: The Authors.

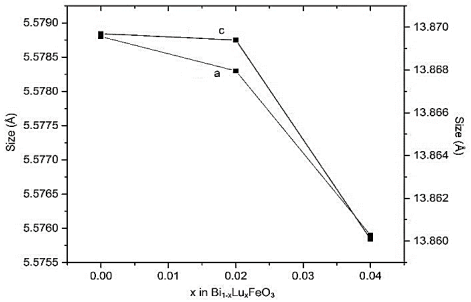

Figure 4. Lattice parameters as a function of x in the $Bi_{1-x}Lu_xFeO_3$ system.
Source: The Authors.

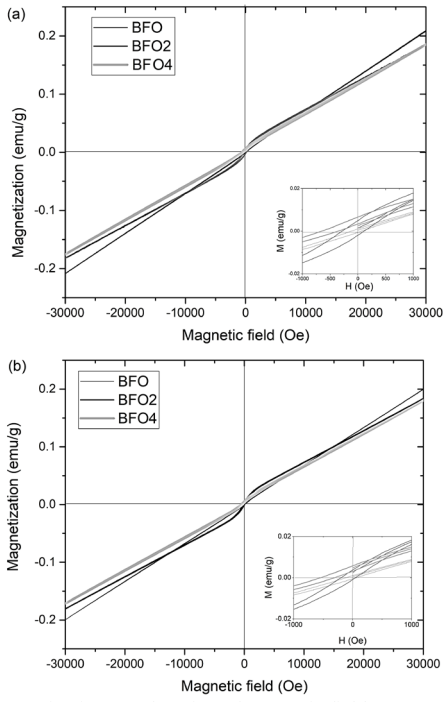

Figure 5. Magnetization as a function of magnetic field (a) 50 K and (b) 200 K of the Bi1-x LuxFeO3 samples.
Source: The Authors.

Table 2.
Values of coercive field and remnant magnetization for the $Bi_{1-x}Lu_xFeO_3$ system.

	Temperature (K)	x = 0.00	x = 0.02	x = 0.04
M_r	50	$6.00x10^{-4}$	$3.30x10^{-3}$	$4.20x10^{-3}$
(emu/g)	200	$4.35x10^{-4}$	$1.00x10^{-3}$	$1.13x10^{-3}$
H_c	50	66	187.5	625
(Oe)	200	45	50	127

Source: The Authors.

The results show a linear increase in magnetization in regards to the applied field without magnetic saturation. This is attributed to antiferromagnetic ordering and spin structure in the material [29]. The zoom-in section of hysteresis loops showed a slight ferromagnetic behavior for each material, the small hysteresis loops of $BiFeO_3$ is due to parasitic ferromagnetism caused by the magnetic moments and spin canting effect in the antiferromagnetic network [30,31].

The magnetization results are in accordance with the phases found by XRD. Ferromagnetic ordering is associated with the presence of a secondary phase ($Bi_2Fe_4O_9$) and the antiferromagnetic ordering is caused by the main phase [32].

Magnetization as a function of temperature is shown in Fig. 6. Some transitions occur at two temperatures: at 250 K is presented the typical transition PM-AFM characteristic of bismuth ferrite systems and at 120 K was presented a slight curvature attributed to the lutetium insertion. It should be noted that Lu^{3+} ion is non-magnetic, and Bi^{3+} ion has a low energy multiplet, which can contribute to the Van Vleck-type magnetic susceptibility. Under 120 K, the negative values are due to the susceptibility of the antiferromagnetic phase [33].

Some researches attribute the increase of magnetization to size particle reduction, which is because of enhancing the uncompensated antiferromagnetic spins in the material surface. In contrast, the magnetization increase was not associated with a direct contribution of lutetium, since it is not a magnetic ion. Nevertheless, it was attributed to the high structural stability of the new material and the decrease of the lattice parameters. [34,35].

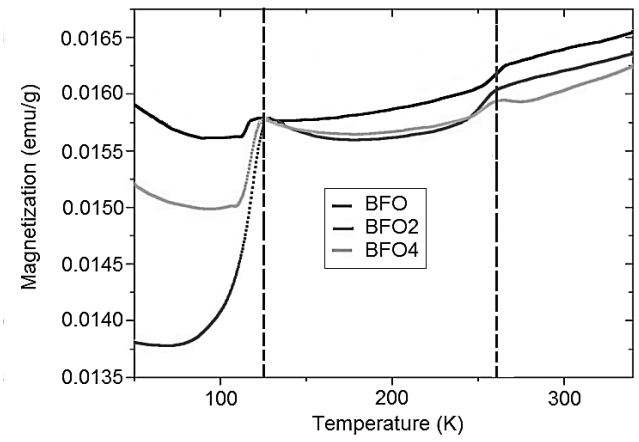

Figure 6. Magnetization as a function of temperature from 50 to 320 K for $Bi_{1-x}Lu_xFeO_3$ samples under 1000 Oe magnetic field.
Source: The Authors.

4. Conclusion

Lutetium doped Bismuth ferrite in low percentages (2% and 4%) was synthesized by solid-state reaction using lower temperatures than those reported in the literature. The materials showed a majority phase of rhombohedral structure and space-group of *R3c* (161) with the presence of the secondary phase ($Bi_2Fe_4O_9$). These results were confirmed by Rietveld refinement, which showed that the insertion of lutetium cation improves structural stability and decreases the lattice parameters. SEM analyzes showed the formation of particles with smaller sizes by increasing the x value, this is due to the small Lu^{3+} ionic radius. The increase of magnetization, allowed to demonstrate that lutetium substitution was performed efficiently and favored the secondary phase diminution and size particle reduction, generating better magnetic properties.

References

[1] Béa, H., Gajek, M., Bibes, M. and Barthélémy, A., Spintronics with multiferroics. Journal of Physics: Condensed Matter, 20(43), pp. 1-11, 2008. DOI: 10.1088/0953-8984/20/43/434221

[2] Catalan, G. and Scott, J.F., Physics and applications of bismuth ferrite. Advanced Materials, 21(24), pp. 2463-2485, 2009. DOI: 10.1002/adma.200802849

[3] Hill, N.A., Why are there so few magnetic ferroelectrics?. Journal of Physical Chemestry B, 29, pp. 6694-6709, 2000. DOI: 10.1021/jp000114x

[4] Mazumder, R., Sujatha-Devi, P., Bhattacharya, D., Choudhury, P., Sen, A. and Raja, M., Ferromagnetism in nanoscale $BiFeO_3$. Applied Physics Letters, 91(6), pp. 1-13, 2007. DOI: 10.1063/1.2768201

[5] Khomchenko, V.A., Troyanchuk, I.O., Kovetskaya, M.I., Kopcewicz, M. and Paixão, J.A., Effect of Mn substitution on crystal structure and magnetic properties of $Bi_{1-x}Pr_xFeO_3$ multiferroics. Journal of Physics D: Applied Physics, 45(4), pp. 1-5, 2012. DOI: 10.1088/0022-3727/45/4/045302

[6] Ederer, C. and Spaldin, N.A., Weak ferromagnetism and magnetoelectric coupling in bismuth ferrite. Physical Review B, 71(6), pp.1-4, 2005.

[7] Mao, W., Wang, X., Han, Y., Li, X. A., Li, Y., Wang, Y. and Huang, W., Effect of Ln (Ln= La, Pr) and Co co-doped on the magnetic and ferroelectric properties of $BiFeO_3$ nanoparticles. Journal of Alloys and Compounds, 584, pp. 520-523, 2014. DOI: 10.1016/j.jallcom.2013.09.117

[8] Singh, H. and Yadav, K.L., Structural, dielectric, vibrational and magnetic properties of Sm doped $BiFeO_3$ multiferroic ceramics prepared by a rapid liquid phase sintering method. Ceramics International, 41(8), pp. 9285-9295, 2015. DOI: 10.1016/j.ceramint.2015.03.212

[9] Khomchenko, V.A., Kiselev, D.A., Bdikin, I.K., Shvartsman, V.V., Borisov, P., Kleemann, W. and Kholkin, A.L., Crystal structure and multiferroic properties of Gd-substituted $BiFeO_3$. Applied Physics Letters, 93(26), pp. 1-3, 2008. DOI: 10.1063/1.3058708

[10] Yuan, G.L., Or, S.W., Liu, J.M. and Liu, Z.G., Structural transformation and ferroelectromagnetic behavior in single-phase $Bi_{1-x}Nd_xFeO_3$ multiferroic ceramics. Applied Physics Letters, 89(5), pp. 1-4, 2006. DOI: 10.1063/1.2266992.

[11] Yuan, G.L. and Or, S.W., Enhanced piezoelectric and pyroelectric effects in single-phase multiferroic $Bi_{1-x}Nd_xFeO_3$ (x = 0–0.15) ceramics. Applied Physics Letters, 88(6), pp. 1-3, 2006. DOI: 10.1063/1.2169905.

[12] Jeon, N., Rout, D., Kim, I. W. and Kang, S.J.L., Enhanced multiferroic properties of single-phase $BiFeO_3$ bulk ceramics by Ho doping. Applied Physics Letters, 98(7), pp. 1-3, 2011. DOI: 10.1063/1.3552682.

[13] Khomchenko, V.A., Karpinsky, D.V., Kholkin, A.L., Sobolev, N.A., Kakazei, G.N., Araujo, J.P. and Paixao, J.A., Rhombohedral-to-orthorhombic transition and multiferroic properties of Dy-substituted $BiFeO_3$. Journal of Applied Physics, 108(7), pp.1-5, 2010. DOI: 10.1063/1.3486500

[14] Varshney, D., Sharma, P., Satapathy, S. and Gupta, P.K., Structural, magnetic and dielectric properties of Pr-modified $BiFeO_3$ multiferroic. Journal of Alloys and Compounds, 584, pp. 232-239, 2014. DOI: 10.1016/j.jallcom.2013.08.159

[15] Lin, Y.H., Jiang, Q., Wang, Y., Nan, C.W., Chen, L. and Yu, J., Enhancement of ferromagnetic properties in $BiFeO_3$ polycrystalline ceramic by La doping. Applied Physics Letters, 90(17), pp. 1-3, 2007. DOI: 10.1063/1.2732182.

[16] Lotey, G.S. and Verma, N.K., Structural, magnetic, and electrical properties of Gd-doped $BiFeO_3$ nanoparticles with reduced particle size. Journal of Nanoparticle Research, 14(3), pp. 1-11, 2012. DOI: 10.1007/s11051-012-0742-7.

[17] Kothari, D., Reddy, V.R., Gupta, A., Meneghini, C. and Aquilanti, G., Dopaje con Eu en cerámicas $BiFeO_3$ multiferroicas estudiadas por Mossbauer y espectroscopía EXAFS. Journal of Physics: Condensed Matter, 22(35), pp. 1-10, 2010. DOI: 10.1088/0953-8984/22/35/356001.

[18] Carvalho, T.T. and Tavares, P.B., Synthesis and thermodynamic stability of multiferroic $BiFeO_3$. Materials Letters, 62(24), pp. 3984-3986, 2008. DOI: 10.1016/j.matlet.2008.05.051

[19] Miao, J.H., Fang, T.T., Chung, H.Y. and Yang, C.W., Effect of La doping on the phase conversion, microstructure change, and electrical properties of $Bi_2Fe_4O_9$ ceramics. Journal of the American Ceramic Society, 92(11), pp. 2762-2764, 2009. DOI: 10.1111/j.1551-2916.2009.03238.x

[20] Gautam, A., Uniyal, P., Yadav, K.L. and Rangra, V.S., Dielectric and magnetic properties of $Bi_{1-x}Y_xFeO_3$ ceramics. Journal of Physics and Chemistry of Solids, 73(2), pp. 188-192, 2012. DOI: 10.1016/j.jpcs.2011.11.005.

[21] Li, Q., Bao, S., Liu, Y., Li, Y., Jing, Y. and Li, J., Influence of lightly Sm-substitution on crystal structure, magnetic and dielectric properties of $BiFeO_3$ ceramics. Journal of Alloys and Compounds, 682, pp. 672-678, 2016. DOI: 10.1016/j.jallcom.2016.05.023

[22] Sati, P.C., Arora, M., Chauhan, S., Kumar, M. and Chhoker, S., Effect of Dy substitution on structural, magnetic and optical properties of $BiFeO_3$ ceramics. Journal of Physics and Chemistry of Solids, 75(1), pp. 105-108, 2014. DOI: 10.1016/j.jpcs.2013.09.003

[23] Tang, P., Kuang, D., Yang, S. and Zhang, Y., The structural, optical and enhanced magnetic properties of $Bi_{1-x}Gd_xFe_{1-y}Mn_yO_3$ nanoparticles synthesized by sol–gel. Journal of Alloys and Compounds, 622, pp. 194-199, 2015. DOI: 10.1016/j.jallcom.2014.10.035

[24] Kumar, A. and Varshney, D., Structural transition and enhanced ferromagnetic properties of La, Nd, Gd, and Dy-doped $BiFeO_3$ ceramics. Journal of Electronic Materials, 44(11), pp. 4354-4366, 2015. DOI: 10.1007/s11664-015-3962-7.

[25] Karthik, T., Rao, T.D., Srinivas, A. and Asthana, S., A-Site Cation disorder and Size variance effects on the physical properties of multiferroic $Bi_{0.9}RE_{0.1}FeO_3$ Ceramics (RE = Gd^{3+}, Tb^{3+}, Dy^{3+}), arXiv preprint, pp. 1-12, 2012. arXiv:1206.5606

[26] Gómez, J.-A., Canaria, C.-C., Burgos, R.-E., Ortiz, C.-A., Supelano, I. and Parra, C.-A., Structural study of yttrium substituted $BiFeO_3$. Journal of Physics: Conference Series, 687(1), pp. 012091, 2016. DOI: 10.1088/1742-6596/687/1/012091.

[27] Londoño, J.-S., Peña, S.-S., Sáchica, E.-H., Pacheco, A.-C., Santos, A. S. and Parra, C.A., Structural and magnetic analysis of the $Bi_{x-1}Sm_xFeO_3$ (x= 0.04 and 0.07) system. Journal of Physics: Conference Series, 935(1), pp. 012007, 2017. DOI: 10.1088/1742-6596/935/1/012007.

[28] Garca, F., Sánchez, F., Cortés, C.A., Barba, A. and Bolarín, A.M., Mechanically assisted synthesis of multiferroic $BiFeO_3$: effect of synthesis parameters. Journal of Alloys and Compounds, 711, pp. 77-84, 2017. DOI: 10.1016/j.jallcom.2017.03.292

[29] Köferstein, R., Synthesis, phase evolution and properties of phase-pure nanocrystalline $BiFeO_3$ prepared by a starch-based combustion method. Journal of Alloys and Compounds, 590, pp. 324-330, 2014. DOI: 10.1016/j.jallcom.2013.12.120

[30] Wang, L., Xu, J.B., Gao, B., Bian, L. and Chen, X.Y., Synthesis of pure phase $BiFeO_3$ powders by direct thermal decomposition of metal nitrates. Ceramics International, 39, pp. S221-S225, 2013. DOI: 10.1016/j.ceramint.2012.10.066

[31] Pedro, F., Betancourt-Cantera, L.G., Bolarín-Miró, A.M., Cortés-Escobedo, C.A., Barba-Pingarrón, A. and Sánchez-De Jesús, F. Magnetoelectric coupling in multiferroic $BiFeO_3$ by co-doping with strontium and nickel. Ceramics International, 45(8), pp. 10114-10119, 2019. DOI: 10.1016/j.ceramint.2019.02.058

[32] Zhao, J., Liu, T., Xu, Y., He, Y. and Chen, W., Synthesis and characterization of $Bi_2Fe_4O_9$ powders. Materials Chemistry and Physics, 128(3), pp. 388-391, 2011. DOI: 10.1016/j.matchemphys.2011.03.011

[33] Layek, S. and Verma, H.C., Magnetic and dielectric properties of multiferroic $BiFeO_3$ nanoparticles synthesized by a novel citrate combustion method, pp. 1-14, 2015.

[34] Gómez, J.-A., Supelano, I, Palacio, C.-A. and Parra, C.-A., Production and structural and magnetic characterization of a $Bi_{1-x}Y_xFeO_3$ (x = 0, 0.25 and 0.30) system. Journal of Physics: Conference Series, IOP Publishing, 614(1), pp. 1-5, 2015. DOI: 10.1088/1742-6596/614/1/012003.

[35] Park, T.J., Papaefthymiou, G.C., Viescas, A.J., Moodenbaugh, A.R. and Wong, S.S., Size-dependent magnetic properties of single-crystalline multiferroic $BiFeO_3$ nanoparticles. Nano letters, 7(3), pp. 766-772, 2007. DOI: 10.1021/nl063039w

A.M. Morales-Rivera, is MSc. in Chemistry from the Universidad Nacional de Colombia, currently works as a researcher in the research group Física de Materiales at Universidad Pedagógica y Tecnológica de Colombia, Tunja, Colombia. There, she works on the synthesis and characterization of advanced ceramic materials.
ORCID: 0000-0003-0300-5280.

I.F. Betancourt-Montañez, is MSc. in Physics student from Universidad Pedagógica y Tecnológica de Colombia, Tunja, Colombia. He is an active member of the research group Fisica de Materiales. He currently works on Materials Science.
ORCID: 0000-0002-4768-8899

S.A. Martínez-Ovalle, is PhD. in Bioengineering and Medical Physics at Universidad Nacional de Colombia. He is a professor at the School of Physics at Universidad Pedagógica y Tecnológica de Colombia, Tunja. He belongs to the research group Física Nuclear Aplicada y Simulación, where he carries out studies in nuclear geophysics, medical physics and radiation protection, and applied nuclear physics.
ORCID: 0000-0003-3044-3008

O.H. Pardo-Cuervo, is PhD. in Chemical Sciences from Universidad Pedagógica y Tecnológica de Colombia, Tunja, currently works as a researcher in the catalysis research group and is also a professor in the Faculty of Science at Universidad Pedagogica y Tecnologica de Colombia, Tunja, Colombia.
ORCID: 0000-0003-4357-404X

J.A. Mejía-Gómez, is PhD. in Physical Sciences from Ghent University, Belgium. She currently works as a professor and researcher at Universidad Antonio Nariño, Tunja, Colombia. Her current research interests include synthesis and characterization of ceramics, thin films, organic compounds and nanomaterials. She is the leader of Grupo de Investigación Fundamental y Aplicada en Materiales- GIFAM.
ORCID: 0000-0002-3737-2153

S. Segura –Peña, is MSc. in Physical Sciences from the Universidad Pedagógica y Tecnológica de Colombia, Tunja, Colombia. She has been a professor in the Department of Basic Sciences at Universidad Santo Tomás, Tunja campus, and a Coordinator of the new materials study line from Grupo de Ciencia Aplicada (GCAT).
ORCID: 0000-0002-3758-8229.

C.A. Ortíz-Otálora, is MSc. in Physics from Universidad Nacional de Colombia. He is a professor at the School of Physics at Universidad Pedagógica y Tecnológica de Colombia, Tunja, Colombia. He is in charge of an X-ray diffractometer and is an active member of the Grupo de Superficies Electroquímica y Corrosión - GSEC.
ORCID: 0000-0003-4943-3707.

C.A. Parra-Vargas, is PhD. in Physical Sciences from Universidad Nacional de Colombia. He is a professor at the School of Physics at Universidad Pedagógica y Tecnológica de Colombia, Tunja, Colombia, where he is also the coordinator of the research group Fisica de Materiales-GFM. He works on materials science.
ORCID: 0000-0001-8968-8654.